4-1-2014

Functionalization of Carbon Nanotube Yarn by Acid Treatment

Heath E. Misak

Ramazan Asmatulu
Wichita State University

Mat O'Malley
Air Force Research Laboratory

Emil Jurak
Wichita State University

Shankar Mall
Air Force Institute of Technology

Recommended Citation

Misak, H. E., Asmatulu, R., O'Malley, M., Jurak, E., & Mall, S. (2014). Functionalization of carbon nanotube yarn by acid treatment. International Journal of Smart and Nano Materials, 5(1), 34–43. https://doi.org/10.1080/19475411.2014.896426

International Journal of Smart and Nano Materials

ISSN: 1947-5411 (Print) 1947-542X (Online) Journal homepage: https://www.tandfonline.com/loi/tsnm20

Functionalization of carbon nanotube yarn by acid treatment

H.E. Misak, R. Asmatulu, M. O'Malley, E. Jurak & S. Mall

To cite this article: H.E. Misak, R. Asmatulu, M. O'Malley, E. Jurak & S. Mall (2014) Functionalization of carbon nanotube yarn by acid treatment, International Journal of Smart and Nano Materials, 5:1, 34-43, DOI: 10.1080/19475411.2014.896426

To link to this article: https://doi.org/10.1080/19475411.2014.896426

International Journal of Smart and Nano Materials, 2014
Vol. 5, No. 1, 34–43, http://dx.doi.org/10.1080/19475411.2014.896426

Taylor & Francis
Taylor & Francis Group

Functionalization of carbon nanotube yarn by acid treatment

H.E. Misak[a], R. Asmatulu[b], M. O'Malley[c], E. Jurak[b] and S. Mall[a]*

[a]*Department of Aeronautics and Astronautics, Air Force Institute of Technology, 2950 Hobson Way, Wright-Patterson AFB, OH 45433-7765, USA;* [b]*Department of Mechanical Engineering, Wichita State University, 1845 Fairmount, Wichita, KS 67260-0133, USA;* [c]*Air Force Research Laboratory, Materials and Manufacturing Directorate, 2941 Hobson Way, Wright-Patterson AFB, OH 45433-7750, USA*

(*Received 1 November 2013; final version received 17 February 2014*)

Carbon nanotube (CNT) yarn was functionalized using sulfuric and nitric acid solutions in 3:1 volumetric ratio. Successful functionalization of CNT yarn with carboxyl and hydroxyl groups (e.g., COOH, COO–, OH, etc.) was confirmed by attenuated total reflectance spectroscopy. X-ray diffraction revealed no significant change to the atomic in-plane alignment in the CNTs; however, the coherent length along the diameter was significantly reduced during functionalization. A morphology change of wavy extensions protruding from the surface was observed after the functionalization treatment. The force required to fracture the yarn remained the same after the functionalization process; however, the linear density was increased (310%). The increase in linear density after functionalization reduced the tenacity. However, the resistivity density product of the CNT yarn was reduced significantly (234%) after functionalization.

Keywords: carbon nanotube yarns; functionalization; textile; conductivity

1. Introduction

There is a need in commercial applications for textiles that have high electrical conductivity and low density. These fabrics can be used in many applications such as static charge dissipation, conducting wire, shielding against electromagnetic interference, wearable electronics, etc. [1]. In order to make common textiles conductive, fabrics are coated with polypyrrole that has a resistivity of ~5.56E^{-3} Ohms cm and a density of ~1.44 g/cm^3, which translates to a resistivity density product of ~80,000 nOhms m g/cm^3 [2]. This property is considerably inferior when compared to metals. Iron has a resistivity density product of 757 nOhms m g/cm^3, and the more conductive copper has 150 nOhms m g/cm^3. However, metals are not conducive for use in textile and textile-type applications owing to weight, stiffness, and safety. Thus, carbon nanotube (CNT)-based structures

*Corresponding author. Email: Shankar.Mall@afit.edu
The views expressed in this article are those of the authors and do not reflect the official policy or position of the US Air Force, Department of Defense, or the US Government.

have potential that can bridge this gap when low electrical resistivity and low density in these cases are desirable [3].

A great deal of research has been conducted to create long CNT structures for various technological applications such as conductive textiles. One such method is drawing multitudes of short CNTs into a long yarn [4]. Unfortunately, the mechanical properties of the CNT yarn are not as impressive as an individual CNT [5]. This is due to the fact that CNT yarn is made up of multitudes of short CNTs, so the mechanical properties are constrained by the forces required to move one CNT relative to other. Thus, weaker mechanical interlocking and van der Waals forces between CNTs play an important role in fracture resistance of CNT yarn, and not strong covalent bonding as is seen in an individual CNT. Also, the yarn density and the large difference between Young's modulus in tension and Young's modulus in compression play an important role in the mechanical properties of CNT yarn [6–8]. Much success in improving mechanical properties has been linked to the optimization of the CNT drawing process parameters [9,10]. Zhong et al. have used transmission electron microscopy and X-ray diffraction (XRD) studies to characterize how CNTs collapse, thus increasing the density and potential benefits of mechanical interlocking [11]. Gui et al. have studied the control of macro- and microstructure of CNT-based structures for applications including mechanical energy absorption [12].

Others have tried to improve the properties of CNT yarns by secondary treatments after the drawing process. Xiao et al. functionalized CNTs in the yarn by drawing the yarn through barium nitrate. The barium-functionalized yarn performed well as cathodes at high temperatures (1317 K) [13]. Trakakis et al. functionalized buckypaper by oxidation and epoxidation reactions [14]. The oxidation created a denser buckypaper, while the epoxidation created a more foam-like structure. Also, they found that the mechanical and electrical properties increased with higher density. Wei et al. made a CNT/polyvinyl alcohol (PVA) composite yarn with a reported 2.2 GPa tensile strength by utilizing oxygen plasma process to functionalize the CNT ribbon and then dipping in a PVA solution [15]. Malik et al. also made CNT/PVA composite but in the form of a sheet, and the manufacturing process is discussed in detail in [16]. Carretero-González et al. modified CNT yarn by chemically unzipping the CNTs to form nanoribbons of graphene. The resulting nanoribbon yarn has very high specific capacitance properties [17]. Jang et al. also produced nanoribbons by unzipping CNTs to use as point emitters for high current field emission [18].

In this study, CNT yarn was functionalized via sulfuric acid and nitric acid treatment in3:1 volumetric ratio. The treated and non-treated CNTs were characterized by attenuated total reflectance (ATR) module connected to a Fourier transform infrared spectroscopy, scanning electron microscopy (SEM), and XRD. The resistance, tensile strength, and mass of the prepared samples were measured for the treated and non-treated CNT yarns.

2. Experiments

2.1. Materials

CNT yarn was procured from the Nanocomp Technologies, Inc., Concord, New Hampshire, USA. The CNT 1 yarn has a linear density of 0.98 ± 0.10 tex. Tex is the linear density commonly used in textile applications where the density of the fiber can change depending on the packing factor and has the unit of g/km. Acid treatment of the as-received CNT yarn was performed by submerging 100 mm yarn segments into a 3:1 volumetric solution of sulfuric acid and nitric acid for 35 min under slight tension. Slight tension was applied to hinder the yarn from unraveling, however this still occurred to a little extent. The 35 min soak time was chosen based on a preliminary experiment where the resistance of the wire in the bath was

measured and was found to increase significantly after 35 min. Following acid treatment, the yarn was dipped in deionized water multiple times to remove the residue acid.

2.2. Experiments

2.2.1. Linear density

A Mettler Toledo XP26 microbalance (Schaffhausen, Switzerland) was used to determine the mass of the CNT yarn specimens. The measured mass from 100 mm length was used to find the linear density (g/km or tex) for each specimen. An accurate cross-sectional area of the yarns was difficult to determine due to the varying degrees of CNT packing factors, micro- and nanoscale gaps/voids, and properties that are dependent on processing parameters. For example, since CNTs are tubular structures, there is a gap inside. A yarn has ribbon–ribbon boundaries that would also produce micro gaps [19]. Thus, presentation of the strength properties in terms of tenacity (N/tex) is more appropriate and allows the yarns to be readily compared to other studies and fabrication methods. Tenacity, linear density, and density will be mentioned often henceforth. For clarification, tenacity is force divided by linear density (N/tex), linear density is weight divided by length (g/km), and density is weight divided by volume (g/cm^3).

2.2.2. Tensile test

The CNT yarn specimens were tested until they fractured under a monotonic tensile loading condition using an Agilent T150 UTM test machine with a 500 mN load cell. CNT yarn specimens with a gauge length of 100 mm were glued between two thin pieces of plastic and inserted into the grips. On both ends, the CNT yarn was glued in between 2 thin 20 mm long plastic pieces. The gauge length was 100 mm. The specimens were pulled at a strain rate of 0.001 mm/(mm sec)).

2.3. Resistance

Resistance was measured before and after the process of functionalization. A four-point probe technique was used to measure the electrical resistivity using a Keithley 2400 SourceMeter (Cleveland, OH, USA) with a current of 0.1 A. A jig was used to ensure that the distance between each probe was 1 cm when measuring resistivity.

As stated previously, it is difficult to accurately determine the cross-sectional area of CNT yarn due to nanoscale gaps and varying packing density of CNTs. Resistivity density product ($\rho \times d$) is independent of area as seen below:

$$\rho \times d = R\frac{A_1}{\ell} \times \frac{m}{LA_1} \tag{1}$$

$$\rho \times d = R\frac{m}{\ell L} \tag{2}$$

where ρ is resistivity, d is density, A_1 is cross-sectional area of the yarn, R is resistance along the length (ℓ) of the yarn, and m is mass of yarn of length L of the CNT yarn. Furthermore, presenting the resistivity density product provided a convenient and consistent comparison among different materials.

2.4. Characterization tests

The CNT yarn was characterized via three different methods: ATR, SEM, and XRD. Thermo Nicolet Avatar 360 (Madison, WI, USA) with SmartPerformer ATR accessory was used for ATR. A Quanta 450 (Brno-Královo Pole, Czech Republic) SEM set at 2 kV acceleration voltage with a spot size of 2.5 was used to image the CNT yarn. XRD tests were performed using a Bruker D2 Phaser (Fitchburg, WI, USA; 30 kV, 10 mA) equipped with sealed Cu X-ray tube (λ = 1.54178 Å) and a Lynxeye linear position sensitive detector. The XRD data were collected with a 0.05° step size at 1 sec dwell time. For these measurements, CNT yarn was cut into 1 cm length samples which were spread out on zero background specimen holders, off-axis silicon. A split Pearson VII function was used to calculate the peak positions and full width at half maxima.

3. Results and discussion

3.1. ATR tests

The CNT yarn was tested using ATR spectroscopy in air with a slight mechanical pressure placed above the yarn to flatten the yarn against the ATR crystal. The results obtained from the ATR spectroscopy test can be seen in Figure 1. Figure 1(a) shows the results for the as-received yarn. As expected, the pure CNTs made up of carbon show very little signal. Carbon strongly absorbs infrared light in a broad range of frequencies making it difficult to resolve the details. Also note that the spectrum is flat from 2500 to 3600 cm^{-1}, which shows there are no hydroxyl groups in the as-received specimen.

Figure 1(b) shows the results for the functionalized CNT yarn. Two peaks are detected at 1140 and 1030 cm^{-1}, which is typical of C–O and C–O–C stretching that were due to the inherent impurities in the as-received CNTs. A strong peak at 1700 cm^{-1} confirms the existence of the C=O bond and the broad peak around 3400 cm^{-1} confirms the existence of the OH bond stretching. Based on the test results, it can be concluded that the CNT yarns were successfully functionalized with carboxyl and hydroxyl groups (e.g., COOH, COO–, OH, etc.), and the results are consistent with other studies conducted on CNT powders [20,21]. The CNTs reacted with nitric acid solution to form carboxyl functional groups on the CNT yarn. This reaction is as follows:

$$\mathrm{CNT} + \mathrm{HNO_3} \xrightarrow{\mathrm{H^+}} \mathrm{CNT} - \mathrm{COO^-} + \mathrm{NO_2} + \mathrm{H_2O} \rightarrow \mathrm{CNT} - \mathrm{COOH} \tag{3}$$

3.2. Morphology analysis

There was a significant morphology change due to the functionalization of the CNT yarn. The morphology of the as-received CNT yarn can be seen in Figure 2(a). The yarn has a smooth

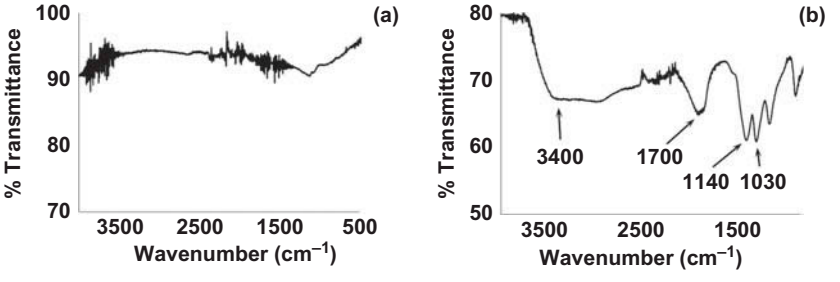

Figure 1. ATR results of (a) as-received and (b) treated CNT yarn.

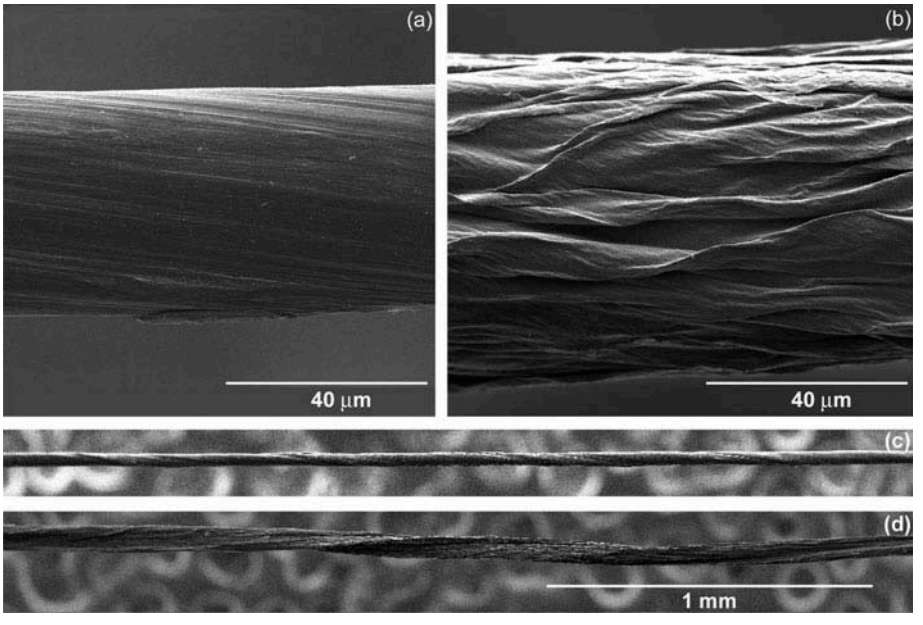

Figure 2. SEM image of (a, c) as-received and (b, d) functionalized CNT yarn.

surface and a slight twist along the longitudinal axis. After functionalization (Figure 2(b)), the surface still has a smooth appearance, but new wavy extensions protrude out of the surface. Furthermore, the functionalized CNT yarn (Figure 2(c)) reverts back to the ribbons of CNTs, as can be seen in Figure 2(d). This morphology change can be explained by hydrophobic interactions, van der Waals and capillary force interactions between the CNTs, and functional group repulsions (or charge repulsions) [22]. There are many voids/porosity through which the solution can seep into the yarn by capillary force and can rearrange the CNT structure.

3.3. XRD tests

3.3.1. (001) Peak

XRD was used to analyze the crystalline nature of individual CNTs in the CNT yarn before and after the functionalization process as shown in Figure 3. The first peak at 25.9°

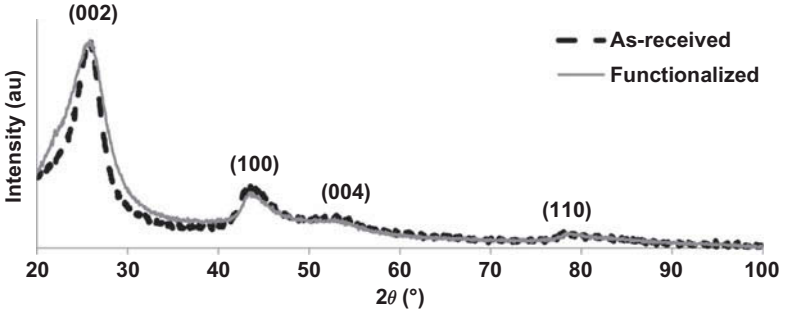

Figure 3. XRD pattern of as-received and functionalized CNT yarn.

is identified as the (002) peak that is commonly seen due to the spacing between graphitic layers in carbon-based materials. Utilizing Bragg's law, the distance between these layers, or more specifically the distance between individual CNTs in the MWCNT ($d_{(002)}$-spacing) can be determined. The (002) d-spacing was found to be 3.42 Å, which is congruent with the accepted value [23] for CNTs.

From Figure 3, it can be seen that the functionalized CNT yarn (002) peak is considerably broader than the counterpart from the as-received yarn. The increase in broadening likely occurs due to an increased strain between graphic layers as well as partial reduction in the number of layers (walls) as a result of the functionalization process. Thus, it can be concluded that the 35min exposure to the sulfuric and nitric acid solutions in 3:1 volumetric ratio created significant defects disrupting the $d_{(002)}$-spacing and resulting in peak broadening.

3.3.2. (100) Peak

The (100) peak represents the curved graphene sheets that make up the structure of MWCNTs [23]. The (100) peak intensity is affected by diffractions from in-plane regularity. Based on the data in Figure 3, it can be seen that once the (002) peaks are normalized to each other, there is a limited decrease in intensity from the (100) peak after the functionalization process. This shows that functionalization did not catastrophically affect the in-plane regularity due to translation, twisting, or altering the helicity between tubes in a given CNT. Also, the shape of the (100) peak broadening was comparable for both, which suggests no appreciable reduction in the size of the nanotubes or increased strain along the length of the nanotubes due to functionalization. Further, the fact that (100) peak did not decrease in intensity proves that the CNTs did not chemically unzip into nanoribbons.

3.4. Functionalization

The electrical and mechanical properties were tested for the as-received and the functionalized CNT yarns. As described earlier, the area of a CNT yarn is difficult to calculate due to voids and surface irregularities. Thus, the data are reported in the form of resistivity density product. Figure 4 shows the resistivity density product for the as-received and functionalized CNT yarn. There is a significant decrease in the resistivity density product, i.e., from 2860 to 1224 nOhms m g/cm^3, after the functionalization process. This

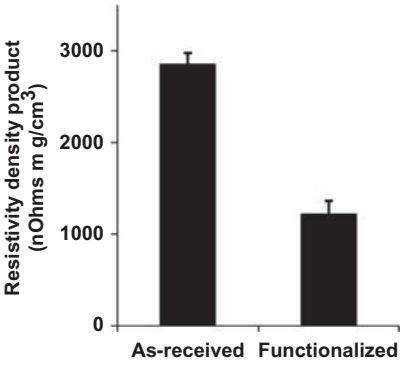

Figure 4. Resistivity density product of as-received and functionalized CNT yarns.

corresponds to a 234% decrease in resistivity density product. Further, the functionalized CNT yarn is highly conductive among the textile/woven fibers. For example, fabrics, which are commonly coated with polypyrrole, have resistivity density product of ~80,000 nOhms m g/cm^3 [2]. Thus, the functionalized CNT yarn is a better conductive material compared to the commonly used textile materials coated with polypyrrole. On the other hand, the resistivity density product of the functionalized CNT yarn is slightly higher than that of metals, e.g., resistivity density product of iron and copper are 757 and 150 nOhms m g/cm^3, respectively.

A linear density is commonly used in textiles to assess their strength, i.e., strength is expressed in terms of tenacity (N/tex or N km/g). This is because the packing factor of fibers in the yarn can vary depending on the manufacturing process and parameters. The packing factor can significantly alter the physical and mechanical properties. Figure 5 shows the linear density (tex = g/km) of CNT yarn. From the chart, the linear density of the as-received and functionalized CNT yarn is 0.98 ± 0.10 and 3.04 ± 0.15 tex, respectively. This 310% increase in linear weight is not only due to the addition of oxygen and hydrogen from the functionalization process but also due to the contraction of the yarn. Upon soaking in the acid bath, the yarns untwist to form a ribbon-type shape from a cylinder, thus changing its geometry along with contraction in length.

Unlike resistivity density product, there is a considerable decrease in tenacity after the functionalization process. As shown in Figure 6, the tex of the as-received CNT yarn

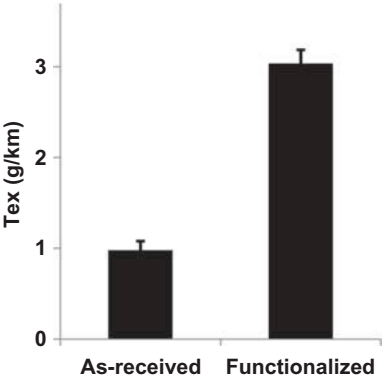

Figure 5. Tex of as-received and functionalized CNT yarns.

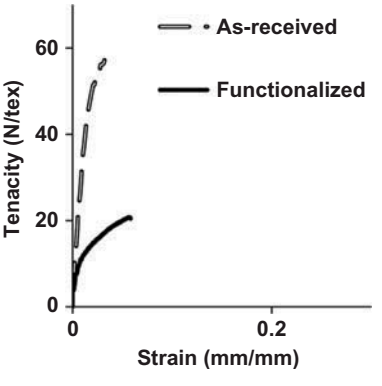

Figure 6. Tenacity versus strain of as-received and functionalized CNT yarns.

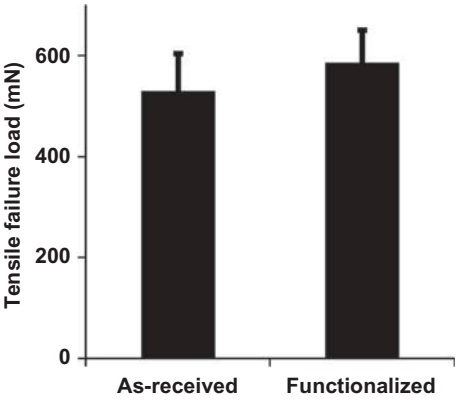

Figure 7. Tensile force of as-received and functionalized CNT yarns.

changed from 55 ± 5.2 to 21 ± 2.1 N/tex after functionalization of the CNT yarn. However, the actual failure loads of the as-received and functionalized CNT yarns were almost comparable (Figure 7). This indicates that the functionalization process had practically no effect on the tensile failure load directly, but the tenacity value was significantly reduced due to an increase in the weight. As a CNT yarn is made up of multitudes of CNTs, the limiting factor involved in tensile strength is the force required to slide one CNT past the other, and not the tensile strength of the individual CNT. Therefore, functional groups did not appear to increase mechanical interlocking within the yarn that would prevent sliding between CNTs and increase strength; however, the conductivity increased (resistivity density products decreased) due to the functional groups which increased the mobility of electrons within the CNT yarn.

4. Conclusion

CNT yarns were successfully functionalized with carboxyl and hydroxyl groups (e.g., COOH, COO–, OH, etc.) by submerging the CNTs into a 3:1 volumetric bath of sulfuric and nitric acid solutions for 35 min. During the submersion of the CNT yarn into the acid bath, the yarn's morphology changed from a smooth surface to a smooth surface with wavy extensions protruding from the surface. Also, the twisted yarn partially untwisted into a yarn ribbon. The functionalization of the individual CNT did not significantly change the in-plane regularity, however, after 35 min of exposure to the acid bath created significant atomic defects that disrupted the atomic pattern along the length of the diameter. The functionalization process increased the linear density by 310% and resistivity density product by 234%. The functionalized CNT yarn has superior resistivity density product (1224 nOhms m g/cm^3) when compared to conventional conductive coatings of polypyrrole (80,000 nOhms m g/cm^3). CNT yarn is a promising conductive fabric material.

References

[1] L. Hu, M. Pasta, F.L. Mantia, L. Cui, S. Jeong, H.D. Deshazer, J.W. Choi, S.M. Han, and Y. Cui, *Stretchable, porous, and conductive energy textiles*, Nano Letters. 10 (2010), pp. 708–714. doi:10.1021/nl903949m

[2] R. Technology, and R.T.L. Smithers Rapra Ltd, *Polymers in Electronics 2007*, iSmithers Rapra Publishing, Shawbury, 2007.
[3] M.F.L. De Volder, S.H. Tawfick, R.H. Baughman, and A.J. Hart, *Carbon nanotubes: Present and future commercial applications*, Science 339 (2013), pp. 535–539. doi:10.1126/science.1222453
[4] K. Jiang, Q. Li, and S. Fan, *Nanotechnology: Spinning continuous carbon nanotube yarns*, Nature 419 (2002), p. 801. doi:10.1038/419801a
[5] V. Sabelkin, H.E. Misak, S. Mall, R. Asmatulu, and P.E. Kladitis, *Tensile loading behavior of carbon nanotube wires*, Carbon 50 (2012), pp. 2530–2538. doi:10.1016/j.carbon.2012.01.077
[6] H.E. Misak, V. Sabelkin, S. Mall, R. Asmatulu, and P.E. Kladitis, *Failure analysis of carbon nanotube wires*, Carbon 50 (2012), pp. 4871–4879. doi:10.1016/j.carbon.2012.06.015
[7] H.E. Misak, R. Asmatulu, V. Sabelkin, S. Mall, and P.E. Kladitis, *Tension–tension fatigue behavior of carbon nanotube wires*, Carbon 52 (2013), pp. 225–231. doi:10.1016/j.carbon.2012.09.024
[8] H.E. Misak, V. Sabelkin, S. Mall, and P.E. Kladitis, *Thermal fatigue and hypothermal atomic oxygen exposure behavior of carbon nanotube wire*, Carbon 57 (2013), pp. 42–49. doi:10.1016/j.carbon.2013.01.028
[9] X. Zhang, K. Jiang, C. Feng, P. Liu, L. Zhang, J. Kong, T. Zhang, Q. Li, and S. Fan, *Spinning and processing continuous yarns from 4-inch wafer scale super-aligned carbon nanotube arrays*, Adv. Mater. 18 (2006), pp. 1505–1510. doi:10.1002/adma.200502528
[10] C.D. Tran, W. Humphries, S.M. Smith, C. Huynh, and S. Lucas, *Improving the tensile strength of carbon nanotube spun yarns using a modified spinning process*, Carbon 47 (2009), pp. 2662–2670. doi:10.1016/j.carbon.2009.05.020
[11] X.H. Zhong, R. Wang, L.B. Liu, M. Kang, Y.Y. Wen, F. Hou, J.M. Feng, and Y.L. Li, *Structures and characterizations of bundles of collapsed double-walled carbon nanotubes*, Nanotechnology 23 (2012), p. 505712. doi:10.1088/0957-4484/23/50/505712
[12] X. Gui, Z. Lin, Z. Zeng, K. Wang, D. Wu, and Z. Tang, *Controllable synthesis of spongy carbon nanotube blocks with tunable macro- and microstructures*, Nanotechnology 24 (2013), p. 085705. doi:10.1088/0957-4484/24/8/085705
[13] L. Xiao, P. Liu, L. Liu, K. Jiang, X. Feng, Y. Wei, L. Qian, S. Fan, and T. Zhang, *Barium-functionalized multiwalled carbon nanotube yarns as low-work-function thermionic cathodes*, Appl. Phys. Lett. 92 (2008), p. 153108. doi:10.1063/1.2909593
[14] G. Trakakis, D. Tasis, J. Parthenios, C. Galiotis, and K. Papagelis, *Structural properties of chemically functionalized carbon nanotube thin films*, Materials 6 (2013), pp. 2360–2371. doi:10.3390/ma6062360
[15] H. Wei, Y. Wei, Y. Wu, L. Liu, S. Fan, and K. Jiang, *High-strength composite yarns derived from oxygen plasma modified super-aligned carbon nanotube arrays*, Nano Res. 6 (2013), pp. 208–215. doi:10.1007/s12274-013-0297-7
[16] R. Malik, Y. Song, N. Alvarez, B. Ruff, M. Haase, B. Suberu, A. Gilpin, M. Schulz, and V. Shanov, *Atmospheric pressure plasma functionalization of dry-spun multi-walled carbon nanotubes sheets and its application in CNT–polyvinyl alcohol (PVA) composites*, MRS Online Proceedings Library 1574 (2013). Available at http://iopscience.iop.org/0957-4484/24/8/085705.
[17] J. Carretero-González, E. Castillo-Martínez, M. Dias-Lima, M. Acik, D.M. Rogers, J. Sovich, C.S. Haines, X. Lepró, M. Kozlov, A. Zhakidov, Y. Chabal, and R.H. Baughman, *Oriented graphene nanoribbon yarn and sheet from aligned multi-walled carbon nanotube sheets*, Adv. Mater. 24 (2012), pp. 5695–5701. doi:10.1002/adma.201201602
[18] E.Y. Jang, J. Carretero-González, A. Choi, W.J. Kim, M.E. Kozlov, T. Kim, T.J. Kang, S.J. Baek, D.W. Kim, Y.W. Park, R.H. Baughman, and Y.H. Kim, *Fibers of reduced graphene oxide nanoribbons*, Nanotechnology 23 (2012), p. 235601. doi:10.1088/0957-4484/23/23/235601
[19] H.E. Misak and S. Mall, *Investigation into microstructure of carbon nanotube multi-yarn*, Carbon (2014, in press). Available at http://dx.doi.org/10.1016/j.carbon.2014.02.012. doi:10.1016/j.carbon.2014.02.012.
[20] Y.-S. Kim, J.-H. Cho, S. Ansari, H.-I. Kim, M. Dar, H.-K. Seo, G.-S. Kim, D.-S. Lee, G. Khang, and H.-S. Shin, *Immobilization of avidin on the functionalized carbon nanotubes*, Synth. Met. 156 (2006), pp. 938–943. doi:10.1016/j.synthmet.2006.06.003

[21] T. Ramanathan, F.T. Fisher, R.S. Ruoff, and L. Catherine Brinson, *Apparent enhanced solubility of single-wall carbon nanotubes in a deuterated acid mixture*, J. Nanotechnol. 2008 (2008), 4p. Article ID 296928.
[22] R. Asmatulu and R.H. Yoon, *Effects of surface forces on dewatering of fine particles*, in *Separation Technologies for Minerals, Coal and Earth Resources*, C. Young and G.H. Luttrell., eds., Society for Mining Metallurgy, and Explorations (SME), Englewood, CO, 2012, pp. 95–102.
[23] P.J.F. Harris, *Carbon Nanotube Science: Synthesis, Properties and Applications*, Cambridge University Press, Cambridge, 2009.